Journal of the Physical Society of Japan **91**, 044005 (2022)
https://doi.org/10.7566/JPSJ.91.044005

Quantum-inspired Search Method for Low-energy States of Classical Ising Hamiltonians

Hiroshi Ueda[1,2,3], Yuichi Otsuka[2,4], and Seiji Yunoki[2,4,5,6]

[1]*Center for Quantum Information and Quantum Biology, Osaka University, Toyonaka, Osaka 560-0043, Japan*
[2]*Computational Materials Science Research Team, RIKEN Center for Computational Science (R-CCS), Kobe 650-0047, Japan*
[3]*JST, PRESTO, Kawaguchi, Saitama 332-0012, Japan*
[4]*Quantum Computational Science Research Team, RIKEN Center for Quantum Computing (RQC), Wako, Saitama 351-0198, Japan*
[5]*Computational Condensed Matter Physics Laboratory, RIKEN Cluster for Pioneering Research (CPR), Wako, Saitama 351-0198, Japan*
[6]*Computational Quantum Matter Research Team, RIKEN Center for Emergent Matter Science (CEMS), Wako, Saitama 351-0198, Japan*

(Received November 1, 2021; accepted January 31, 2022; published online March 17, 2022)

We develop a quantum-inspired numerical procedure for searching low-energy states of a classical Hamiltonian composed of two-body fully connected random Ising interactions and a random local longitudinal magnetic field. In this method, we introduce infinitesimal quantum interactions that do not commute with the original Ising Hamiltonian and repeatedly generate and truncate direct product states, following the idea of the Krylov subspace method, to obtain the low-energy states of the original classical Ising Hamiltonian. The computational cost is controlled by the form of infinitesimal quantum interactions (e.g., one- or two-body interactions) and the numbers of infinitesimal interaction terms introduced, different initial states considered, and low-energy states kept during the iteration. For a demonstration of the method, here, we introduce pair products of Pauli X operators acting on different sites and on-site Pauli X operators into the random Ising Hamiltonian as the infinitesimal quantum interactions, in which the computational cost is $O(N^3)$ per iteration with the system size N. We consider 120 instances of the random coupling realizations for the random Ising Hamiltonian with N up to 600 and search the 120 lowest-energy states for each instance. We find that the time-to-solution by the quantum-inspired method proposed here, with parallelization in terms of the different initial states, for searching the ground state of the random Ising Hamiltonian scales approximately as N^5 for N up to 600. We also examine the basic physical properties such as the ensemble-averaged ground-state and first-excited energies and the ensemble-averaged number of states in the low-energy region of the random Ising Hamiltonian.

1. Introduction

There has been renewed interest in quantum annealing (QA)[1–8] particularly because of the successful development of the first commercially available real quantum device for QA by D-Wave Systems in 2011.[9] It is indeed noteworthy that the appearance and usage of QA devices have strongly evoked potential needs of solving discrete optimization problems for practical applications to industrial and social problems. Although the optimization problem is, in general, very difficult to solve if we insist on finding the best solution, there are many cases where suboptimal solutions can beneficially serve practical purposes, provided that these solutions are obtained within a reasonable computational time. This is, in fact, the case for the D-Wave devices because they have advantages in finding (near-)optimal solutions much faster than classical computers,[10] even though it is difficult to ensure that the best solution is always obtained because of finite temperature effects and other sources of noise.

Most of the discrete optimization problems can be described as a problem of finding the ground state of a classical Ising model[11] given by the following Hamiltonian:

$$\hat{H}_0 = \sum_{i<j} J_{ij}\hat{\sigma}_i^z\hat{\sigma}_j^z + \sum_i h_i\hat{\sigma}_i^z, \tag{1}$$

where $\hat{\sigma}_i^z$ is a Pauli-Z operator for a spin at site i. The problem of finding the ground state of the Ising model for general J_{ij} and h_i is NP-hard,[12–14] and it is known as the spin glass in statistical physics.[15]

Simulated annealing (SA)[16] was developed as a numerical technique to address this problem, and it exploits thermal fluctuation to effectively select the ground state among many candidates. QA is a quantum analogy of SA, in which quantum fluctuation instead of a thermal one is utilized as a driving force for the annealing process. Note that QA has nowadays also been studied as a kind of a quantum adiabatic optimization approach in the context of near-term gate-based quantum computers.[17] In QA, we introduce an additional Hamiltonian $\hat{H}_1$ with $[\hat{H}_0, \hat{H}_1] \neq 0$, whose ground state is easily obtained numerically or experimentally. We then construct a time-dependent Hamiltonian $\hat{H}(\tau)$ within a time interval of $\tau = [0, \tau_0]$,

$$\hat{H}(\tau) = \left(1 - \frac{\tau}{\tau_0}\right)\hat{H}_1 + \frac{\tau}{\tau_0}\hat{H}_0, \tag{2}$$

and consider the real-time evolution $|\Psi(\tau)\rangle = T_\tau \exp[\frac{1}{i\hbar}\int_0^\tau \hat{H}(\tau')\,d\tau']|\Psi(0)\rangle$, where $|\Psi(0)\rangle$ is the trivial ground state of $\hat{H}_1$ at $\tau = 0$ and $T_\tau[\cdot]$ denotes the time-ordered product. The advantage of QA is that the adiabatic theorem for quantum systems[18–21] guarantees that the ground state of $\hat{H}_0$ is, in principle, obtained as the final state of this process for sufficiently large τ_0, unless there occurs a level crossing between the ground state and excited states of $\hat{H}(\tau)$ during the entire process. Even if $\hat{H}(\tau)$ undergoes a first-order phase transition in the thermodynamic limit, we can modify $\hat{H}(\tau)$ by, for example, adding another quantum Hamiltonian[22,23] to avoid the transition.

While the annealing approaches allow for a general and efficient way to find the ground state of the Hamiltonian $\hat{H}_0$,

note that the ground state of the Ising model does not always yield the solution of the original optimization problem if the problem includes constraint conditions. The constraint conditions are usually incorporated in the Ising model of Eq. (1) with associated hyperparameters, which cannot be determined a priori. We need to verify whether the ground state estimated by a searching algorithm satisfies the constraint conditions; if not, we may repeat the searching algorithm or tune the hyperparameters. These repeating and/or tuning processes can be computationally demanding. On the other hand, if we can obtain a number of low-energy states of the Ising model at once, the above process can be simplified because one might expect that the feasible solution that satisfies the constraint conditions is found in the low-energy excited states of the mapped Hamiltonian $\hat{H}_0$.

For some difficult optimization problems, e.g., those with hard constraints, it is expected that feasible solutions cannot be found near the ground state of the Ising model. Nevertheless, we expect that knowledge of a number of candidate solutions is informative when tuning the hyperparameters or, at least, judging how the optimization problem under consideration is difficult. For example, it has recently been proposed that a history of the repeating process of the single search is valuable for optimizing the hyperparameter.[24] However, it is not obvious which is efficient in general, repeating the single search or finding a number of candidates at once, being highly dependent on the specific problem.

In this paper, we propose a quantum-inspired (QI) method for finding a number of low-energy states of the classical Ising Hamiltonian $\hat{H}_0$ in Eq. (1) with random couplings J_{ij} and h_i. In this algorithm, we generate classical direct product states by introducing an infinitesimal quantum interaction $\hat{H}_1$ and subsequently truncate those states with higher energies, which constitute a single iteration. We then repeat this procedure until the predetermined condition is satisfied, thus obtaining the desired number of lowest-energy states. This procedure is based on the idea of the Krylov subspace method,[25] known as one of the most successful algorithms in numerical linear algebra. The computational cost and accuracy are controlled by the choice of $\hat{H}_1$ and the numbers of iterations, initial classical states, and states kept. For a demonstration, we consider all possible pair products of Pauli X operators acting on different sites and on-site Pauli X operators as $\hat{H}_1$, and show that the computational cost scales as N^3 per iteration with N being the total number of Ising spins. We take 120 different instances of the random coupling J_{ij} and h_i realizations for each N up to 600, and search the 120 lowest-energy states for each random coupling instance to examine the scalability of the proposed QI search method. Additionally, we discuss the basic properties of the random Ising model such as the ensemble-averaged ground-state and first-excited energies and the ensemble-averaged number of states in the low-energy region of $\hat{H}_0$.

The rest of this paper is organized as follows. We first introduce the physical background of the QI search method proposed here in Sect. 2 and describe the algorithm for the search of low-energy states of the classical Ising model $\hat{H}_0$ in Sect. 3. We then analyze the efficiency of the algorithm for searching the 120 lowest-energy states, including the ground state, of $\hat{H}_0$ in Sect. 4. We also discuss the basic physical properties of $\hat{H}_0$ obtained by the QI search method and other methods in Sect. 5. The summary and conclusion are finally provided in Sect. 6. The performances of the QI search method and the parallel-tempering Monte Carlo (PTMC) method are compared in Appendix.

2. Physical Background of QI Search Method

The QI search method can be formulated as a classical limit of the M-block two-step Krylov subspace method, which is a variant of the two-step Lanczos method.[26] In this section, first, we briefly review the M-block two-step Krylov subspace method to calculate the M lowest eigenenergies and the corresponding eigenstates of a given Hamiltonian,

$$\hat{H}_{\rm tot} = \hat{H}_0 + \lambda \hat{H}_1, \tag{3}$$

where $\hat{H}_0$ and $\hat{H}_1$ are noncommuting classical and quantum Hamiltonians, respectively, as introduced in Sect. 1, and λ is a coupling constant. We assume the eigenvalues E_ψ of H_0 in the ascending order with $0 \le \psi < 2^N$ and the corresponding classical eigenstates $|\psi\rangle$, i.e., $\hat{H}_0|\psi\rangle = E_\psi|\psi\rangle$.

In the M-block two-step Krylov subspace method, we first prepare M random orthonormal classical states $\{|i\rangle := |\psi_i\rangle\}_{1\le i\le M}$ with $0 \le \psi_i < 2^N$, which are eigenstates of $\hat{H}_0$, i.e.,

$$\hat{H}_0|i\rangle = E_{\psi_i}|i\rangle, \tag{4}$$

with the eigenvalues E_{ψ_i} in the ascending order $E_0 \le E_{\psi_1} \le \cdots \le E_{\psi_M}$. Next, we generate M quantum states,

$$|\phi_i\rangle := \hat{H}_{\rm tot}|i\rangle, \tag{5}$$

and using, for example, the modified Gram–Schmidt orthonormalization, we orthonormalize these resulting states $|\phi_i\rangle$ as well as the states $|i\rangle$ to obtain the following $2M$ orthonormal states:

$$|\phi'_j\rangle := \begin{cases} |j\rangle & 1 \le j \le M \\ |\tilde{\phi}_{j-M}\rangle & M+1 \le j \le 2M \end{cases}, \tag{6}$$

where the state $|\tilde{\phi}_{j-M}\rangle$ is proportional to $|\phi_{j-M}\rangle - \sum_{j'<j}\langle\phi'_{j'}|\phi_{j-M}\rangle|\phi'_{j'}\rangle$.

After the orthonormalization, we next construct the following $2M$-dimensional effective Hamiltonian

$$\hat{H}'_{\rm tot} := \sum_{j,j'=1}^{2M} \langle\phi'_j|\hat{H}_{\rm tot}|\phi'_{j'}\rangle|\phi'_j\rangle\langle\phi'_{j'}|, \tag{7}$$

and diagonalize this Hamiltonian $\hat{H}'_{\rm tot}$ to obtain the $2M$ eigenenergies $\{E'_j\}$ in the ascending order with the corresponding eigenstates $\{|\Phi_j\rangle\}$, i.e.,

$$\hat{H}'_{\rm tot}|\Phi_j\rangle = E'_j|\Phi_j\rangle. \tag{8}$$

We then set $|i\rangle := |\Phi_i\rangle$ for $i = 1, 2, \ldots, M$ as the initial states in Eq. (5) and repeat the above procedure in Eqs. (5)–(8) until the M lowest eigenenergies E'_j converge within the desired accuracy. In this way, the M-block two-step Krylov subspace method can be used to compute not only the ground-state energy but also the low-lying excited-state energies, which is the advantage over the standard (one-block) Krylov subspace method. The M-block two-step Krylov subspace method can be applied to any quantum system if one can store $2M$ vectors of length 2^N. However, it is clearly impossible for large N since the dimension of vector grows exponentially with N, resulting in the memory

bottleneck. Therefore, we need an approximation for large N and, hence, we consider a classical limit of the M-block two-step Krylov subspace method using only classical basis sets, where merely $O(M \sim \mathrm{poly}(N))$ coefficients should be kept in the memory.

As in the M-block two-step Krylov subspace method, we first prepare the orthonormal M initial classical states $\{|i\rangle\}$. We then expand the set of classical states by following the guiding principle of the Krylov subspace method, i.e.,

$$\{|\psi'_k\rangle\}_{1\le k\le K} := \{|\psi\rangle; \langle\psi|\hat{H}_{\mathrm{tot}}|i\rangle \neq 0\}. \tag{9}$$

In a typical system in condensed-matter physics, including the Ising model described by the Hamiltonian in Eq. (1), the number of K is up to $O(N^2)$ because the quantum Hamiltonian $\hat{H}_1$ consists of only local n-body spin flip terms with n typically up to 2. Here we assume that the classical states $|\psi'_k\rangle$ with $\psi'_k \in [0, 2^N)$ are ordered ascendingly with respect to k, i.e., $E_{\psi'_1} \le E_{\psi'_2} \le \cdots \le E_{\psi'_K}$. Next, these K-dimensional basis states are used to construct the following effective Hamiltonian:

$$\hat{H}'_{\mathrm{tot}} := \sum_{k,k'=1}^{K} \langle\psi'_k|\hat{H}_{\mathrm{tot}}|\psi'_{k'}\rangle|\psi'_k\rangle\langle\psi'_{k'}|, \tag{10}$$

which is diagonalized to obtain the eigenenergies $\{E'_k\}_{1\le k\le K}$ in the ascending order and the corresponding eigenstates $\{|\Psi_k\rangle\}_{1\le k\le K}$, i.e.,

$$\hat{H}'_{\mathrm{tot}}|\Psi_k\rangle = E'_k|\Psi_k\rangle. \tag{11}$$

For the next iteration, as the initial classical states $|i\rangle$ in Eq. (9), we select M ($< K$) classical states for approximating the M' ($\le M$) lowest eigenstates $\{|\Psi_{i'}\rangle\}_{1\le i'\le M'}$; if we focus only on the ground state, we adopt $M' = 1$. The selection of the states is made on the basis of the following quantity:

$$p_{M',k} := \langle\psi'_k|\left(\frac{1}{M'}\sum_{i'=1}^{M'}|\Psi_{i'}\rangle\langle\Psi_{i'}|\right)|\psi'_k\rangle. \tag{12}$$

Namely, we select M classical states $|\psi'_k\rangle$ that represent M largest values among $\{p_{M',k}\}_{1\le k\le K}$. Using these classical states as the initial states $|i\rangle$ in Eq. (9), we repeat the above procedure until the M lowest eigenenergies $\{E'_k\}_{1\le k\le M}$ in Eq. (11) converge within the desired accuracy.

Assuming that $\lambda \ll 1$ and the classical states $|\psi'_k\rangle$ are not degenerate, one can simply use the lowest-order perturbation theory to approximately solve the eigenvalue problem in Eq. (11), i.e.,

$$|\Psi_k\rangle = |\psi'_k\rangle + \lambda\sum_{k'(\neq k)}^{K}|\psi'_{k'}\rangle\frac{\langle\psi'_{k'}|\hat{H}_1|\psi'_k\rangle}{E_{\psi'_k} - E_{\psi'_{k'}}} \tag{13}$$

and

$$E'_k = E_k + \lambda^2\sum_{k'(\neq k)}^{K}\frac{|\langle\psi'_{k'}|\hat{H}_1|\psi'_k\rangle|^2}{E_{\psi'_k} - E_{\psi'_{k'}}}. \tag{14}$$

Therefore, in the limit of the infinitesimal perturbation, the selection of the M classical states based on $p_{M',k}$ is identical to the selection of the M classical states having the M lowest eigenenergies $\{E_{\psi'_k}\}_{1\le k\le M}$, implying that the evaluation of $\hat{H}'_{\mathrm{tot}}$ and its diagonalization are not required. This argument can be generalized even when there exist degenerate classical states. Hence, in the classical limit of the Krylov subspace method, we can search the low-energy states of $\hat{H}_0$. This is the main physical idea of the QI search method and more details are described in the next section. The success probability of the QI search method can be improved by increasing M or by optimizing the form of the quantum Hamiltonian $\hat{H}_1$. Here, we choose as $\hat{H}_1$ one- and two-body spin flipping terms, namely, $\hat{\sigma}^x_i$ and $\hat{\sigma}^x_i\hat{\sigma}^x_j$ for all possible sites i and pairs of sites i and j with $i \neq j$, respectively.

3. Algorithm

In this section, we describe algorithms for the QI search method in detail. First, we introduce $|\sigma\rangle \in \{|0\rangle, |1\rangle\}$ as a complete set of a local spin state, which are eigenstates of the Pauli-Z operator, i.e., $\hat{\sigma}^z|0\rangle = |0\rangle$ and $\hat{\sigma}^z|1\rangle = -|1\rangle$. Using this local basis set, we can express any state for the N-spin system as $|\boldsymbol{\sigma} = (\sigma_0, \ldots, \sigma_{N-1})\rangle$, which forms the complete set of states. For the fast simulation in the classical computer, we employ a typical form of the state list that makes a one-to-one correspondence between the vector $\boldsymbol{\sigma}$ and an integer ψ representing a state as follows:

$$|\psi\rangle \equiv |\boldsymbol{\sigma}\rangle \text{ with } \psi = (\sigma_{N-1}\cdots\sigma_1\sigma_0)_2 = \sum_{i=0}^{N-1}2^i\sigma_i. \tag{15}$$

Next, as a basic operation in the search algorithm, we define a procedure to obtain the ℓ-site spin-flipped state $|\psi'\rangle = \prod_{k=1}^{\ell}\hat{\sigma}^x_{i_k}|\psi\rangle$ for a given state $|\psi\rangle$ with $1 \le \ell \le N$ and $0 \le i_1 < \cdots < i_\ell < N$. Here, $\hat{\sigma}^x_i$ is the Pauli-X operator for the ith-site spin. For this operation, we employ the bitwise exclusive or operation (BITXOR), as shown in Algorithm 1.

Algorithm 1 Multiple spin flips for an N-site system

Input: integer ψ in Eq. (15), ℓ with $1 \le \ell \le N$, and $\boldsymbol{i} = (i_1, \ldots, i_\ell)$ with $0 \le i_1 < \cdots < i_\ell < N$.
Output: integer ψ' with $0 \le \psi' < 2^N$.

```
function MULTIPLE_SPIN_FLIP(ψ, i, ℓ)
  x := Σ_{k=1}^{ℓ} 2^{i_k}
  ψ' := BITXOR(x, ψ)
end function
```

The core function for the update of the state lists in the search algorithm is given in Algorithm 2. Let us now assume that we have already kept the $(K+1)$-dimensional integer vector $\boldsymbol{\psi}$ and the $(K+1)$-dimensional real-valued vector $\boldsymbol{E}$ specifying, respectively, $K+1$ classical product states $\{|\psi_i\rangle\}_{1\le i\le K+1}$ and the corresponding energies $\{E_i = \langle\psi_i|\hat{H}_0|\psi_i\rangle\}_{1\le i\le K+1}$, where the order of integers $\psi_1, \psi_2, \ldots, \psi_{K+1}$ is sorted so that $E_1 \le E_2 \le \cdots \le E_{K+1}$. Let us also assume that we have already kept the $(K+1)$-dimensional logical vector $\boldsymbol{l} = \{l_i\}_{1\le i\le K+1}$ with $l_i \in \{\mathrm{True}, \mathrm{False}\}$ to judge whether ψ_i has already been used as an input ψ for Algorithm 2. In addition, for the binary search of a state, we also have the $(K+1)$-dimensional integer vector $\boldsymbol{\psi}'$ whose elements are the same as those of $\boldsymbol{\psi}$ but are sorted in ascending order. In Algorithm 2, we input a state $|\psi\rangle$ at the starting point and perform spin flips to generate a new state $|\psi'\rangle$. If $|\psi'\rangle \notin \boldsymbol{\psi}'$ and the energy $E = \langle\psi'|\hat{H}_0|\psi'\rangle$ is smaller than E_{K+1}, then we update the lists $\boldsymbol{\psi}$, $\boldsymbol{\psi}'$, $\boldsymbol{l}$, and $\boldsymbol{E}$ by discarding $|\psi_{K+1}\rangle$ and E_{K+1}.

Having described Algorithm 2 for updating the state lists, we now provide the main part of the algorithm for the QI single search method in Algorithm 3. In order to perform this algorithm, we have to prepare the set of integers $\mathcal{I}$ for specifying the spin flip operations considered in $\hat{H}_1$. For

Algorithm 2 Update state lists

Input: integer ψ, ℓ, $\boldsymbol{i}$, K with $1 \le K < 2^N$, $\boldsymbol{\psi} = \{\psi_i\}_{1\le i\le K+1}$, and $\boldsymbol{\psi}' = \{\psi'_i\}_{1\le i\le K+1}$ with $0 \le \psi'_1 < \cdots < \psi'_{K+1} < 2^N$; real $\boldsymbol{E} = \{\langle\psi_i|\hat{H}_0|\psi_i\rangle\}_{1\le i\le K+1}$ with $E_1 \le \cdots \le E_{K+1}$; logical variable $\boldsymbol{l} = \{l_i\}_{1\le i\le K+1}$

Output: integer $\boldsymbol{\psi}$ and $\boldsymbol{\psi}'$; real $\boldsymbol{E}$; logical variable $\boldsymbol{l}$

function UPDATE_LIST($\psi, \boldsymbol{i}, \ell, \boldsymbol{\psi}, \boldsymbol{\psi}', \boldsymbol{E}, \boldsymbol{l}, K$)
  $\psi' :=$ MULTIPLE_SPIN_FLIP($\psi, \boldsymbol{i}, \ell$)
  $(p, f) :=$ BINARY_SEARCH($\psi', \boldsymbol{\psi}', K$)
  ▷ The function "BINARY_SEARCH($x, \boldsymbol{x}, K$)" with an integer/real number x and a $(K+1)$-dimensional ascending-ordered integer/real vector $\boldsymbol{x}$ returns an integer p for $x_p \le x < x_{p+1}$ and a logical variable f, which becomes True when $x_p = x$.
  if $f =$ False **then**
    $E := \langle\psi'|\hat{H}_0|\psi'\rangle$
    $(\boldsymbol{\psi}, \boldsymbol{\psi}', \boldsymbol{E}, \boldsymbol{l}) :=$ UPDATE_LIST_SUB($\psi', E,$ False$, p, \boldsymbol{\psi}, \boldsymbol{\psi}', \boldsymbol{E}, \boldsymbol{l}, K$)
  end if
end function

function UPDATE_LIST_SUB($\psi', E, l, p', \boldsymbol{\psi}, \boldsymbol{\psi}', \boldsymbol{E}, \boldsymbol{l}, K$)
  if $E < E_{K+1}$ **then**
    $(p, f) :=$ BINARY_SEARCH($\psi_{K+1}, \boldsymbol{\psi}', K$)
    if $p > p'$ **then**
      $\boldsymbol{\psi}' = (\psi'_1, \ldots, \psi'_{p'}, \psi', \psi'_{p'+1}, \ldots, \psi'_{p-1}, \psi'_{p+1}, \ldots, \psi'_{K+1})$
    else
      $\boldsymbol{\psi}' = (\psi'_1, \ldots, \psi'_{p-1}, \psi'_{p+1}, \ldots, \psi'_{p'}, \psi', \psi'_{p'+1}, \ldots, \psi'_{K+1})$
    end if
    $(p, f) :=$ BINARY_SEARCH($E, \boldsymbol{E}, K$)
    $\boldsymbol{E} := (E_1, \ldots, E_p, E, E_{p+1}, \ldots, E_K)$
    $\boldsymbol{\psi} := (\psi_1, \ldots, \psi_p, \psi', \psi_{p+1}, \ldots, \psi_K)$
    $\boldsymbol{l} := (l_1, \ldots, l_p, l, l_{p+1}, \ldots, l_K)$
  end if
end function

Algorithm 3 QI single search method

Input: integer $N > 0$, ψ, $J > 0$, K, $I > 0$, $\boldsymbol{n} = \{n_j\}_{1\le j\le J}$ with all $n_j > 0$, and a set of $\mathcal{I} = \{\mathbf{I}_j\}_{1\le j\le J}$, where $\mathbf{I}_j = \{\boldsymbol{i}_n^{(j)}\}_{1\le n\le n_j}$ with j-dimensional ascending-ordered integer vector $\boldsymbol{i}_n^{(j)}$

Output: integers $\boldsymbol{\psi}$ and $\boldsymbol{\psi}'$; real $\boldsymbol{E}$; logical variable $\boldsymbol{l}$

function QI_SEARCH($N, \psi, J, K, I, \boldsymbol{n}, \mathcal{I}$)
  ▷ $I_{\rm M}/R_{\rm M}$: the maximum integer/real number that can be expressed in a computer.
  $E := \langle\psi|\hat{H}_0|\psi\rangle$
  $\boldsymbol{\psi} = \{\psi_i\}_{1\le i\le K+1}$; $\psi_i := \begin{cases} \psi & i = 1 \\ I_{\rm M} & \text{otherwise} \end{cases}$
  $\boldsymbol{E} = \{E_i\}_{1\le i\le K+1}$; $E_i := \begin{cases} E & i = 1 \\ R_{\rm M} & \text{otherwise} \end{cases}$
  $\boldsymbol{\psi}' := \boldsymbol{\psi}$
  $\boldsymbol{l} = \{l_i\}_{1\le i\le K+1}$; $\{l_i\} :=$ False
  for $i = 1$ to I **do**
    $f :=$ False
    for $k = 1$ to $K+1$ **do**
      if $l_k =$ False **then**
        $\psi := \psi_k$; $l_k :=$ True; $f :=$ True; **Exit**
      end if
    end for
    if $f =$ True **then**
      for $j = 1$ to J **do**
        for $n = 1$ to n_j **do**
          $(\boldsymbol{\psi}, \boldsymbol{\psi}', \boldsymbol{E}, \boldsymbol{l}) :=$ UPDATE_LIST($\psi, \boldsymbol{i}_n^{(j)}, j, \boldsymbol{\psi}, \boldsymbol{\psi}', \boldsymbol{E}, \boldsymbol{l}, K$)
        end for
      end for
    end if
  end for
end function

Algorithm 4 QI multiple search method

Input: integer $L > 0$, N, J, K, I, $\boldsymbol{n}$, and $\mathcal{I}$

Output: integer $\boldsymbol{\psi}$; real $\boldsymbol{E}$

function QI_MULTI_SEARCH($L, N, J, K, I, \boldsymbol{n}, \mathcal{I}$)
  $\boldsymbol{\phi} = \{\phi_i\}_{1\le i\le L}$; $\phi_i :=$ RAND_BETWEEN$(0, 2^N - 1)$
    ▷ The function RAND_BETWEEN(a, b) returns a randomly selected integer uniformly distributed in the range $[a, b]$.
  $(\boldsymbol{\psi}, \boldsymbol{\psi}', \boldsymbol{E}, \boldsymbol{l}) :=$ QI_SEARCH($N, \phi_1, J, K, I, \boldsymbol{n}, \mathcal{I}$)
  for $i = 2$ to L **do**
    $(\boldsymbol{\psi}_0, \boldsymbol{\psi}'_0, \boldsymbol{E}_0, \boldsymbol{l}_0) =$ QI_SEARCH($N, \phi_i, J, K, I, \boldsymbol{n}, \mathcal{I}$)
    for $j = 1$ to $K+1$ **do**
      $(p, f) :=$ BINARY_SEARCH($\psi'_{0,j}, \boldsymbol{\psi}', K$)
      If $f =$ False **then**
        $(\boldsymbol{\psi}, \boldsymbol{\psi}', \boldsymbol{E}, \boldsymbol{l}) :=$ UPDATE_LIST_SUB($\psi'_{0,j}, E_{0,j}, l_{0,j}, p, \boldsymbol{\psi}, \boldsymbol{\psi}', \boldsymbol{E}, \boldsymbol{l}, K$)
      end if
    end for
  end for
end function

example, when $\hat{H}_1$ contains all patterns of J-spin flips up to $J = 2$, we set the input parameters as follows: $n_1 = N$, $\mathbf{I}_1 = \{\boldsymbol{i}_1^{(1)} = (0), \boldsymbol{i}_2^{(1)} = (1), \ldots, \boldsymbol{i}_{n_1}^{(1)} = (N-1)\}$, $n_2 = N(N-1)/2$, and $\mathbf{I}_2 = \{\boldsymbol{i}_1^{(2)} = (0,1), \boldsymbol{i}_2^{(2)} = (0,2), \ldots, \boldsymbol{i}_{n_2}^{(2)} = (N-2, N-1)\}$. We also input the number K of states kept, the number I of iterations, and ψ for specifying the initial classical state of the calculation.

As we shall show in the next section, the QI single search method is accidentally trapped in a local minimum, depending on the combination of the initial state ψ and the random coupling realization in $\hat{H}_0$. One of the simplest solutions to avoid trapping in a local minimum is to perform the independent QI single searches in parallel for different random initial states and merge the lists obtained from the independent searches. The QI multiple search method given in Algorithm 4 is based on this strategy.

Let us now consider the computational complexity of Algorithm 4. The total number of the spin flip operations required per iteration is $\sum_j n_j \sim O(N^J)$. For a spin-flipped classical state, we have to evaluate the energy of $\hat{H}_0$, which costs naively $O(N^2)$. However, since we know the energy of the state before the spin flip operation, the computational cost for evaluating the energy of the state after the spin flip operation is reduced to $O(N)$ because we only take into account the couplings associated with the spin-flipped sites. The computational cost of searching a state via the binary search is $\log_2 K$, and thus it is negligible because we consider the case for $K \ll 2^N$. Therefore, the leading order of the computational cost per iteration with the system size N is $O(N^{J+1})$. The total computational cost in Algorithm 4 is thus $O(LIN^{J+1})$. In this study, we set the parameters as $(K, I, L) = (K_0, K_0, 1)$ and (K_0, N, N) with $K_0 = N(N+1)/2 + 1$, and hence the total computational cost in both cases is $O(N^5)$, assuming that $J = 2$.

4. Basic Features of QI Search Method

In this section, we test the method by trying to find the 120 lowest-energy states of the classical Ising model described by the Hamiltonian $\hat{H}_0$ in Eq. (1) with the fully connected random interactions J_{ij} and the random magnetic fields h_i, which are both drawn from a uniform distribution on the interval $[-1/2, 1/2]$. We consider 120 different instances of $\hat{H}_0$ for each system size N to quantitatively estimate the accuracy and efficiency of the QI search method. The results for N up to 30 sites are compared with those obtained exactly

by the brute-force (BF) search. For larger systems with $N \sim O(10^3)$, the results are compared with those obtained by the PTMC method,[27,28] focusing only on the ground-state energy.

4.1 *Numerical setup and elapsed time*

We first investigate the elapsed time of the QI search method given in Algorithm 4 with the following input parameters: $L = 1$ (i.e., equivalent to the QI single search method given in Algorithm 3), $|\phi_1 = 0\rangle \equiv |00\cdots0\rangle$ for the initial classical state, and $K = I = \sum_{j=1}^{2} n_j + 1$ with $\sum_{j=1}^{2} n_j = N + N(N-1)/2 = N(N+1)/2$, where we assume the infinitesimal quantum Hamiltonian

$$\hat{H}_1 = \epsilon\left(\sum_{i<j} \hat{\sigma}_i^x \hat{\sigma}_j^x + \sum_i \hat{\sigma}_i^x\right) \tag{16}$$

with an infinitesimally small real number ϵ. Note that the one- and two-spin flip operations considered in $\hat{H}_1$ correspond to the example for $\mathbf{I}_1$ and $\mathbf{I}_2$, respectively, given in Sect. 3.

According to the discussion toward the end of Sect. 3, we expect that the leading order of the computational cost of the QI search method with these parameters is $O(N^5)$, which clearly has better scalability than $O(2^N)$ for the BF search. To confirm the scalability, we perform the QI search on the HOKUSAI BigWaterfall (CPU: Intel Xeon Gold 6148 2.4 GHz) installed at RIKEN for the same sets of Hamiltonian $\hat{H}_0$ treated in Sect. 5 and measure the averaged elapsed time without any parallelization. As shown in Fig. 1, we confirm that the elapsed time t of the QI search is nicely on the line of $t \sim N^5$ and is shorter than that of the BF search for $N \geq 14$.

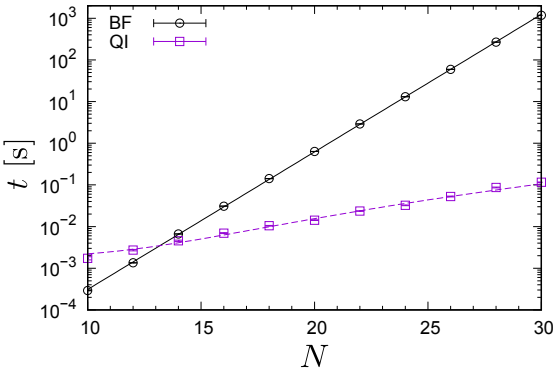

Fig. 1. (Color online) Averaged elapsed time t for the BF search and the QI search with $L = 1$, $K = I = N(N+1)/2 + 1$, $J = 2, n_1 = N$, and $n_2 = N(N-1)/2$ as a function of the system size N. The black solid line and the purple dashed curve are fitting functions $\ln t = a_1 N + b_1$ with $(a_1, b_1) = (0.76, -15.7)$ and $t = a_2 N^5 + b_2$ with $(a_2, b_2) = (4.7 \times 10^{-9}, 1.8 \times 10^{-3})$, respectively.

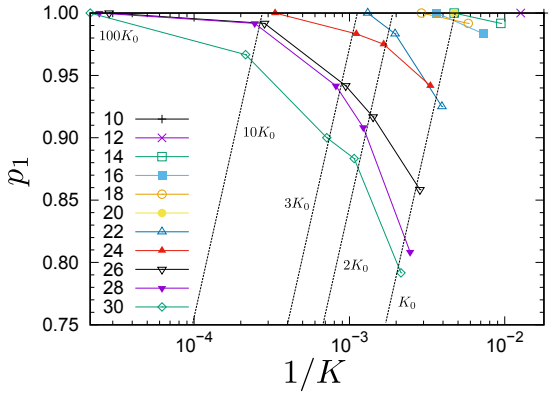

Fig. 2. (Color online) Success probability p_1 of the QI search with $(L, \phi_1) = (1, 0)$ and $I = K$ for different system sizes $N = 10, 12, \ldots, 30$ indicated in the figure. The dotted lines are guides for the eye to highlight the slow decay of the success probability p_1 with increasing N for each $K \in \{K_0, 2K_0, 3K_0, 10K_0, 100K_0\}$ where $K_0 = N(N+1)/2 + 1$.

4.2 *N, L, and K dependences of the success probability for searching the ground state*

As the basic performance of the QI search method, we next investigate the N, L, and K dependences of the success probability p_1 for searching the ground state of the classical Ising Hamiltonian $\hat{H}_0$. Here, p_1 is defined as the ratio between the number of instances of the random coupling realizations in $\hat{H}_0$ for which the ground state is correctly searched and the total number of instances of the random coupling realizations in $\hat{H}_0$, which is 120 for each system size N in this study.

We first perform the QI search by setting the parameters $(L, \phi_1) = (1, 0)$ and $I = K$ for the system sizes up to 30 sites. The number of lowest-energy states kept is set to be $K = aK_0$ with $a \in \{1, 2, 3, 10, 100\}$ and $K_0 = N(N+1)/2 + 1$. We can naively expect that p_1 decreases exponentially with increasing N for a fixed value of a because the number of classical states generated in the QI search for this setting is only $O(IN^2) \sim O(N^4)$, which is extremely smaller than the dimension 2^N of the total Hilbert space. However, as shown in Fig. 2, the probability p_1 decays rather slowly instead of exponentially for each value of a, and rapidly increases to close to 1 with increasing a. These characteristics strongly support the high scalability of the QI search method.

Second, we discuss the efficiency of the QI multiple search with $L > 1$ by setting the input parameters $L = N = 30$, $K = K_0$, and $I \in \{0.1N, 0.2N, 0.3N, 0.5N\}$, where the 30 initial classical states are randomly chosen. To quantify the accuracy and efficiency of the method, here, we estimate a time-to-solution (TTS), that is, the time required to obtain the correct ground state with a successful probability of 0.99.[29–31] The TTS is defined as

$$\mathrm{TTS} = \frac{\ln(1 - 0.99)}{\ln(1 - p_1)} t, \tag{17}$$

where t is the elapsed time of the QI search and we use the averaged elapsed time over 120 instances of the random coupling realizations. Figure 3 shows the results of the TTS for the QI multiple search. For comparison, the results for the QI single search with $N = 30$ (the same results as shown in Fig. 2) are also plotted. Note that the QI single search in Fig. 2 sets $L = 1$ but $I \sim O(N^2)$, while the QI multiple search here sets $L = N$ but $I \sim O(N)$. Hence, the total computational cost is $O(N^5)$ for both cases. Note also that the ground states for all the 120 different instances of the random coupling realizations in $\hat{H}_0$ are found correctly by the QI search with $(I, K, L) = (0.5N, K_0, N)$ and $(100K_0, 100K_0, 1)$, for which the TTS is zero, and thus these results are not plotted in Fig. 3. As shown in Fig. 3, the QI multiple search is already better than the QI single search in this case because the TTS

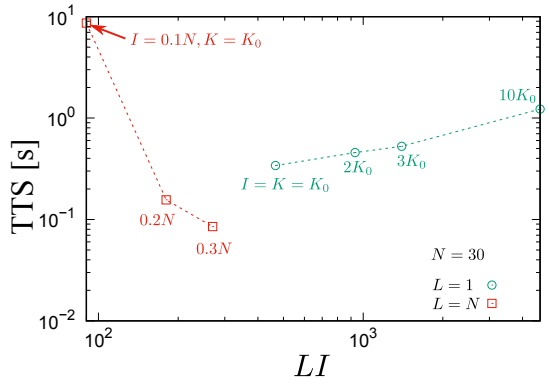

Fig. 3. (Color online) TTS versus the total number of QI iterations, LI, for searching the ground state of 120 different instances of the random coupling realizations in $\hat{H}_0$ with $N = 30$. The QI multiple search method with $L = N$, $K = K_0$, and $I \in \{0.1N, 0.2N, 0.3N, 0.5N\}$ is employed (red squares). For comparison, the results for the QI single search method with $L = 1$, $I = K$, $K \in \{K_0, 2K_0, 3K_0, 10K_0, 100K_0\}$, and $K_0 = N(N+1)/2 + 1$ are also shown by green circles (these results are the same as those shown in Fig. 2). Note that the computational complexity for these two methods with these parameters is $O(N^5)$. The results for $(I, K, L) = (0.5N, K_0, N)$ and $(I, K, L) = (100K_0, 100K_0, 1)$ are not plotted because the TTS is zero.

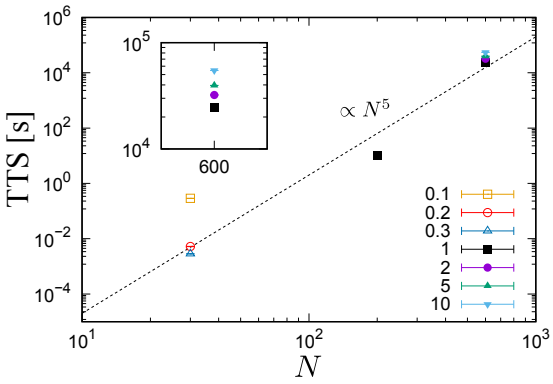

Fig. 4. (Color online) System-size N dependence of the TTS for searching the ground state of 120 different instances of the random coupling realizations in $\hat{H}_0$ with $N = 30$, 200, and 600. Numbers in the legend indicate the value of a for the input parameters $(L, K, I) = (N, aN, aN)$. Inset: enlarged view for the data of $N = 600$. Since the BF search cannot be applied for $N = 200$ and 600, the PTMC method is used to obtain the reference ground-state energy for these large systems (see Appendix).

is smaller, provided that the effective total number of iterations, i.e., LI, is the same. Considering that parallelization of the QI search for different initial states with $L = N$ yields $O(N)$ speed-up, we expect that the TTS for the QI multiple search becomes much smaller, which is clearly a feature advantageous for using supercomputers when the problem size is particularly large.

To confirm the scalability of the QI search method, Fig. 4 shows the results of the TTS for the QI multiple search with OpenMP parallelization in terms of L. Here, we adopt several different input parameters (L, K, I) for the QI search and employ the PTMC method to obtain the reference ground-state energy for large systems. As shown in Fig. 4, we find that the TTS scales approximately as N^5, which is comparable to the scaling of the computational cost $O(N^5)$. The numerical details for larger systems and the comparison with the PTMC results are described in Appendix.

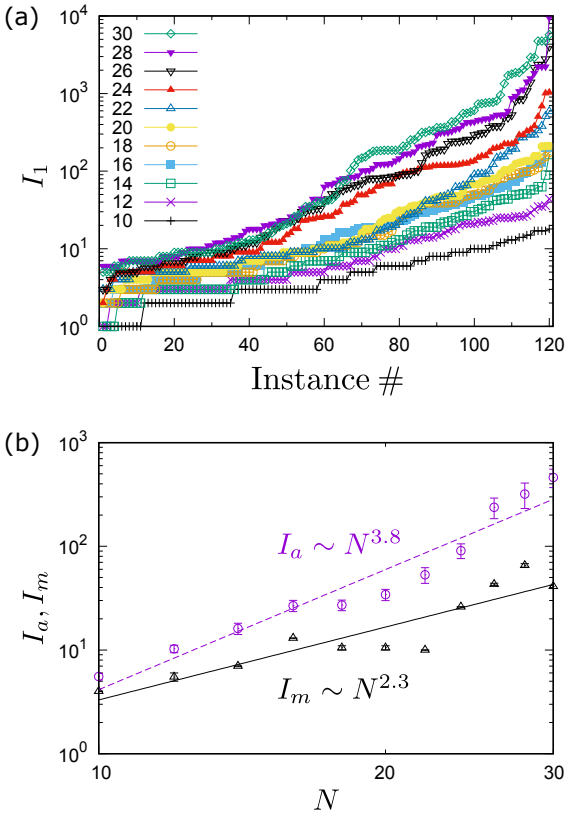

Fig. 5. (Color online) (a) Instance dependence of the number I_1 of iterations required to find the correct ground state of the Hamiltonian $\hat{H}_0$ for 120 different instances of the random coupling realizations with the system size $N = 10, 12, \ldots, 30$ indicated in the figure. Note that the instance number is ordered so that I_1 monotonically increases for each N. (b) Ensemble-averaged I_1 (named I_a) and the median of the ensemble-dependent I_1 (named I_m) as a function of the system size N. The solid and dashed lines are power law fittings of I_m and I_a, respectively.

4.3 Instance and initial state dependence of the number of iterations required for searching the ground state

To understand the reason why the QI multiple search method with $L > 1$ improves the success probability p_1, we now focus on the instance and initial state dependence of the number I_1 of iterations necessary to find the correct ground state of $\hat{H}_0$.

For this purpose, we first employ the QI single search method with the input parameters $(L, \phi_1) = (1, 0)$ and $I = K$ for K up to $100K_0$. Figure 5(a) shows the results of I_1 for 120 different instances of the random coupling realizations in $\hat{H}_0$ with different system sizes. In this figure, the instance number is reordered so that I_1 monotonically increases. We find that I_1 basically increases with the system size N. To capture a feature of this increase, we also evaluate the ensemble-averaged I_1, named I_a, and the median of the ensemble-dependent I_1, named I_m, as a function of N. As shown in Fig. 5(b), we find that $I_a > I_m$ for all system sizes. This is simply because I_1 around instance #120 shown in Fig. 5(a) is particularly larger than that for other instances. In accordance with the results in Fig. 2, I_a and I_m do not seem to increase exponentially with N. Therefore, as shown in Fig. 5(b), we fit I_a and I_m with power law functions and find that the exponent of N for I_m is smaller than that for I_a. This fitting implies that the ground states of half of the instances (i.e., the Hamiltonian $\hat{H}_0$ with different random coupling realizations)

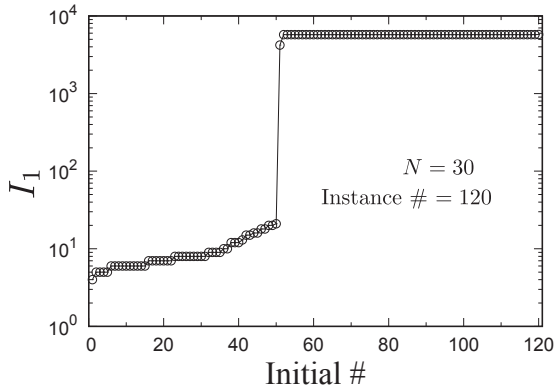

Fig. 6. Initial state dependence of the number I_1 of iterations. The Hamiltonian $\hat{H}_0$ is selected for the random coupling realization of instance #120 in Fig. 5(a) with the system size $N = 30$. The QI single search method is employed with 120 different initial states selected randomly, and the initial number for specifying the different initial states is ordered so that I_1 increases monotonically.

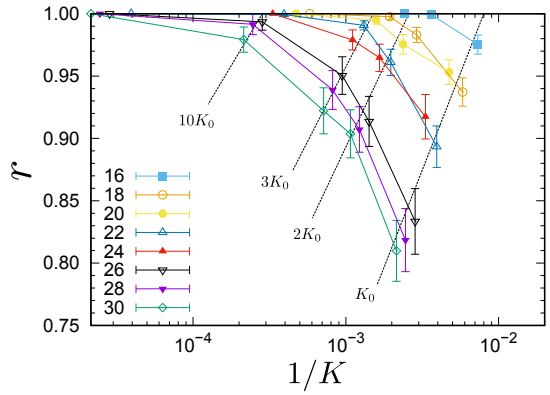

Fig. 7. (Color online) Success rate r of the number of low-energy states successfully detected among the 120 lowest-energy states for a given random coupling realization, which is averaged over 120 different instances of the random coupling realizations in $\hat{H}_0$, with different system sizes $N = 16, 18, \ldots, 30$ indicated in the figure. The error bars indicate the standard error. The QI single search is employed with the input parameters $(L, \phi_1) = (1, 0)$ and $I = K$. The dotted lines are guides for the eye to highlight the slow decay of the success rate r with increasing N for each $K \in \{K_0, 2K_0, 3K_0, 10K_0, 100K_0\}$, where $K_0 = N(N+1)/2 + 1$.

for the system size $N \leq 30$ can be searched successfully with the number of iterations up to only $I_1 \sim O(N^{2.3})$. Having obtained the different exponents, we speculate that the QI single search for the Hamiltonian $\hat{H}_0$ with the random coupling realizations around sample #120 is trapped in a local minimum since, here, we employ only a single initial state with $|\phi_1 = 0\rangle \equiv |00\cdots0\rangle$.

To confirm this assertion, we next explore the initial state dependence of I_1 by performing the QI single search using 120 different initial states for the Hamiltonian $\hat{H}_0$ of instance #120 in Fig. 5(a). Figure 6 shows the results of I_1 as a function of the initial number for specifying the 120 different initial states that are ordered so that I_1 increases monotonically. We find that 40% of the 120 different QI searches can find the ground state successfully with only $I_1 < N$ iterations. This observation clearly supports that the QI multiple search with $L > 1$ is an efficient strategy for avoiding trapping local minima.

4.4 Search efficiency for low-energy excited states

In this section, we shall investigate the efficiency of the QI search for the low-energy excited states. Note that when we perform the QI single search for obtaining the results shown in Fig. 2, K lowest-energy states, in addition to the ground state, are also obtained. This is an advantage of the QI search method proposed in this study. Here, aiming to find 120 lowest-energy states, we evaluate the ensemble-averaged success rate r between the number of states correctly found and the number of the target states, namely, 120. Figure 7 shows the results obtained by the QI single search with the input parameters $(L, \phi_1) = (1, 0)$, $I = K = aK_0$, and $a \in \{1, 2, 3, 10, 100\}$ for N up to 30 sites. Surprisingly, the K dependence of r is very similar to that of the success probability p_1 for searching the ground state shown in Fig. 2. This implies that the QI single search method given in Algorithm 3 is highly scalable not only for the ground state but also for the low-energy excited states.

Figure 8 shows the success rate r versus the averaged elapsed time t for the QI single search with $(L, K, I) = (1, aK_0, aK_0)$ and for the QI multiple search with $(L, K, I) = (N, aK_0, aN)$. The system size is $N = 30$ for both cases. Note that the overall computational costs for these two methods with these parameters both scale as N^5. We find in Fig. 8 that the success rate r for the QI multiple search with $L = N$ is always better than that for the QI single search with $L = 1$, comparing both data for a common averaged elapsed time t. For example, comparison between the result with $a = 2$ for the QI single search and that with $a = 1$ in the QI multiple search, with comparable cost of elapsed time $t \sim 0.2$ s, shows that the error $\epsilon = 1 - r$ of the search in the latter is about 8.3 times smaller than that in the former. We should also emphasize that the QI multiple search with $I = N$ can already find about 99% of the 120 lowest-energy states, and the success rate r becomes even better with larger I. Thus, the QI multiple search with $L > 1$ can efficiently search not only the ground state but also the low-energy excited states.

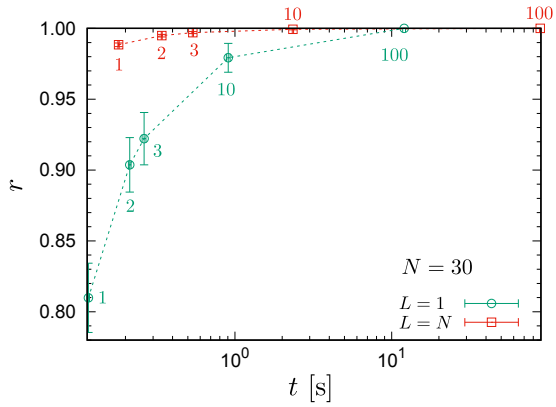

Fig. 8. (Color online) Success rate r versus the elapsed time t for searching the 120 lowest-energy states of $\hat{H}_0$ with the system size $N = 30$. r and t are averaged over 120 different instances of the random coupling realizations in $\hat{H}_0$. The error bars indicate the standard error. The QI single search method with $(L, K, I) = (1, aK_0, aK_0)$ (denoted by green circles) and the QI multiple search method with $(L, K, I) = (N, aK_0, aN)$ (denoted by red squares) are employed. Here, $a \in \{1, 2, 3, 10, 100\}$ and is indicated beside each symbol.

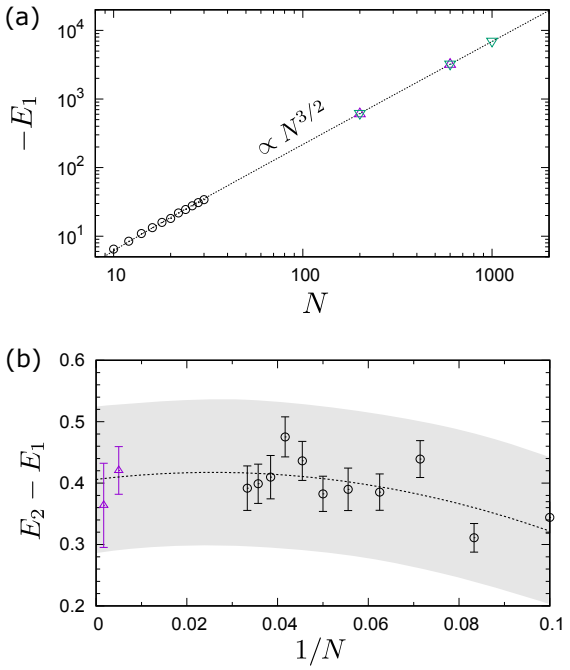

Fig. 9. (Color online) (a) Ensemble-averaged ground-state energy E_1 as a function of the system size N. The results are obtained by the brute-force method (circles), the QI search method (upward triangles), and the PTMC method (downward triangle). The broken line is the fitting function $E_1 = aN^{3/2} + b$ with $a = -0.218 \pm 0.001$ and $b = 0.79 \pm 0.14$. (b) Ensemble-averaged first excitation gap $E_2 - E_1$ as a function of $1/N$ obtained by the BF method (circles) and the QI search method (upward triangles). The error bars indicate the standard error. The dashed line is the quadratic-fit for the gap and the gray shade indicates the fitting error in the thermodynamics limit at $1/N \to 0$. In the cases of $N = 200$ and 600, denoted by upward triangles in (a) and (b), we only use the results of the random coupling instances for which the QI search method and the PTMC method give exactly the same ground-state energy (see Appendix).

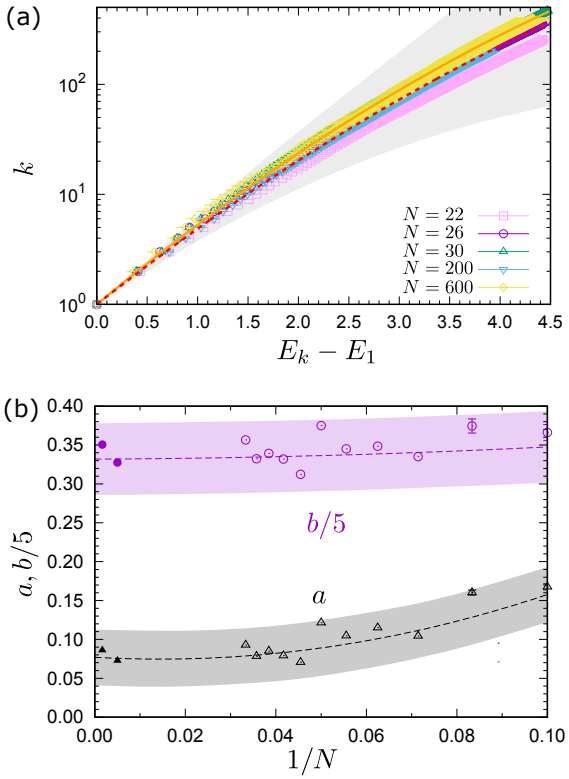

Fig. 10. (Color online) (a) Ensemble-averaged energy difference $E_k - E_1$ between the kth lowest energy E_k and the ground-state energy E_1 with different system sizes up to $N = 600$ (see the text for details of the ensemble). The orange line is the fitting function $\ln k = -a(E_k - E_1)^2 + b(E_k - E_1)$ with $a = 0.0927 \pm 0.0003$ and $b = 1.783 \pm 0.002$ obtained for the results of $N = 30$. The red dashed line is the fitting function in the thermodynamic limit with $a = 0.077 \pm 0.036$ and $b = 1.66 \pm 0.23$ estimated in (b) and the gray shade indicates the fitting error. (b) Fitting parameters a and b as a function of $1/N$. These parameters are obtained by fitting the results of k vs $E_k - E_1$ for each system size N, as in (a). The purple and black dashed lines are the quadratic fits for these parameters a and b, respectively. The purple and gray shades indicate the fitting errors of a and b, respectively, in the thermodynamic limit at $1/N \to 0$.

5. Basic Physical Property of $\hat{H}_0$

Finally, in this section, we briefly study the basic physical properties of the random Ising model described by the Hamiltonian $\hat{H}_0$ in Eq. (1), such as the ground-state and first-excited energies and the number of states in the low-energy region. For this purpose, we employ the QI search method as well as the brute-force method and the PTMC method for system sizes up to $N = 1000$. Note that the Hamiltonian $\hat{H}_0$ with the couplings (J_{ij}, h_i) replaced with $(J_{ij}/\sqrt{N}, 0)$ and J_{ij} being distributed according to the Gaussian distribution is well known as the Sherrington–Kirkpatrick (SK) model,[32] and the ground state of the SK model has been studied by various numerical methods such as genetic algorithms,[33,34] hierarchical methods,[35] extremal optimizations,[36] and conformational space annealing.[37]

To evaluate the physical quantities, we consider 120 instances of the random coupling realizations in $\hat{H}_0$ for each system size N. As in Sect. 4, all the couplings J_{ij} and h_i in $\hat{H}_0$ are chosen randomly from a uniform distribution on the interval $[-1/2, 1/2]$. Figure 9(a) reveals that the ensemble-averaged ground-state energy E_1 is clearly proportional to $N^{3/2}$ and is well fitted by the function $E_1 = aN^{3/2} + b$ with $a = -0.218 \pm 0.001$ and $b = 0.79 \pm 0.14$. The leading exponent $N^{3/2}$ is exactly the same as that of the SK model,[32] taking into account the N dependence of the random couplings in the SK model, i.e., $J_{ij}/\sqrt{N}$. In Fig. 9(b), we also estimate the first excitation gap in the thermodynamic limit by a quadratic fit of the ensemble-averaged first-excited energy $E_2 - E_1$ with respect to $1/N$, and find that there exists a finite gap in the thermodynamic limit as large as $E_2 - E_1 = 0.41 \pm 0.12$.

We also investigate the total number of states $k(E)$ below a certain energy E in the low-energy region. This quantity can be useful, since the first derivative of $k(E)$ with respect to E is related to the density of states. We simply obtain the kth lowest energy E_k, which is averaged over the 120 different instances for $N \leq 30$. For the larger systems with $N = 200$ and 600, we assume that the low-energy states are correctly obtained by the QI search method in the cases where the QI search method and the PTMC method estimate the same ground-state energy. Such cases are found for 95 (26) random coupling instances with $N = 200$ (600), as described in Appendix, and only these results are used for the ensemble average. Figure 10(a) shows the semi-log plot of k vs $E_k - E_1$ in the low-energy region for different system sizes up to $N = 600$. We find that $\ln k$ is almost proportional to $E_k - E_1$ in the vicinity of the ground state $E_k - E_1 \sim 0$ and gradually shifts to an upward-convex function with increas-

ing k. As a phenomenological fitting function, we propose $\ln k = -a(E_k - E_1)^2 + b(E_k - E_1)$ with positive fitting parameters a and b. Applying the least-squares fitting to the date for $N = 30$, we obtain the fitting curve with $a = 0.0927(3)$ and $b = 1.783(2)$, indicated by the orange line in Fig. 10(a), confirming that the fitting curve well fits the data for $E_k - E_1 \leq 4.5$.

Next, we estimate the fitting curve in the thermodynamic limit by first fitting the data of k vs $E_k - E_1$ for each system size N to obtain a and b. Then we perform quadratic fittings of a and b with respect to $1/N$, as shown in Fig. 10(b), and estimate the parameters a and b in the thermodynamic limit by extrapolating them to $1/N \to 0$. The fitting curve with a and b in the thermodynamic limit is indicated by the red dashed line in Fig. 10(a), which is comparable to the data for N up to 600 in the region of $E_k - E_1 \lesssim 1$. Note also that the first-excited energy $E_2 - E_1$ is insensitive to N and it is almost on the red dashed line, thus being consistent with the results shown in Fig. 9(b).

6. Summary and Discussion

We have proposed a QI search method for finding low-energy states of the classical Ising model described by the Hamiltonian $\hat{H}_0$ in Eq. (1) with the random Ising interactions J_{ij} and the random local magnetic fields h_i, to which many discrete optimization problems can be mapped. The main idea of the QI search algorithm is based on a classical limit of the M-block two-step Krylov subspace method, which is known as a powerful method in the numerical linear algebra to calculate the low-energy eigenstates of a matrix. An essential point of the QI search algorithm is to introduce infinitesimal quantum interaction $\hat{H}_1$ that is not commutable to the original classical Hamiltonian $\hat{H}_0$ and expand the Krylov subspace for the total Hamiltonian $\hat{H}_0 + \hat{H}_1$.

The performance of the QI search method is analyzed for the Hamiltonian $\hat{H}_0$ with $\{J_{ij}, h_i\}$ distributed uniformly in the range of $[-1/2, 1/2]$. For this purpose, we considered 120 instances of the random coupling realizations in $\hat{H}_0$. We found that the QI multiple search method given in Algorithm 4 with $L = N$ random initial states can successfully obtain the correct ground states for all the 120 instances with the system size N up to 30 after only $I = N/2$ iterations. In addition, we have shown that 99% of the 120 lowest-energy states are found correctly within $I = N$ iterations. The search accuracy is improved monotonically with increasing number K of states kept and number I of iterations. We have also found that the TTS of the QI search method with OpenMP parallelization for searching the ground state scales approximately as N^5 with the system size N up to 600. The overall computational complexity of the QI search method is $O(LIN^{J+1})$, and the algorithm can be easily parallelized with respect to L, thus making it compatible with the calculations for large systems using supercomputers.

We have also briefly investigated the low-energy properties of the random coupling Ising model described by the Hamiltonian $\hat{H}_0$ using the QI search method as well as the brute-force method and the PTMC method for the system size N up to 1000. We have found that the ensemble-averaged ground-state energy E_1 scales as $N^{3/2}$, which is consistent with the SK model, taking into account the fact that the coupling J_{ij} here is not scaled with N. We have also found that there exists a finite energy gap between the ground state and the first excited state in the thermodynamic limit. Moreover, we have found that the total number $k(E)$ of states below a certain energy E in the low-energy region increases exponentially with the excitation energy.

It would be interesting to explore the search efficiency of the QI search with $\hat{H}_1$ being only the uniform magnetic field $\epsilon \sum_i \hat{\sigma}_i^x$ with $J = 1$. Since the computational cost with $J = 1$ is only $O(N^2)$ in each iteration, comparable to the SA method, we can treat system size up to $O(10^4)$. However, since the number of classical states generated per iteration is only $O(N)$, not $O(N^2)$ as in the case of $J = 2$ considered in this study, we naively expect that the state list is much less updated in the QI search with $J = 1$, assuming the same number of K. As a consequence, the QI search with $J = 1$ may be easily trapped in local minima. Nonetheless, it is worthwhile to perform the QI search with $J = 1$ for the ground-state search of a system size as large as $O(1000)$ and compare the results with other numerical methods such as the SA and PTMC methods; this is left for a future study.

In the classical Ising Hamiltonian $\hat{H}_0$ in Eq. (1), the total $\hat{\sigma}^z$ is a good quantum number. To preserve this symmetry, we can introduce, as the infinitesimal quantum interaction $\hat{H}_1$, the infinitesimal XX interaction $\epsilon \sum_{i<j} (\hat{\sigma}_i^x \hat{\sigma}_j^x + \hat{\sigma}_i^y \hat{\sigma}_j^y)$ by replacing the spin flip operations in Algorithm 1 with the spin exchange operations, and search the ground state and low-energy states for each sector of the total σ^z. Furthermore, the classical Hamiltonian $\hat{H}_0$ considered in statistical physics and condensed-matter physics often has the translational and point group symmetries. We can also implement these symmetry constraints in the QI search algorithm by introducing a representative state for each sector with different quantum numbers associated with the symmetry,[38] which is often used in the exact diagonalization method.

Note that when this method is applied to the Ising model onto which the original optimization problem is mapped, $\hat{H}_1$ is the only nontrivial hyperparameter that is newly introduced in the QI search; other parameters such as the number of iterations and the number of initial classical states should be kept sufficiently large within given computational resources because the search accuracy improves monotonically as they increase. One good strategy to set $\hat{H}_1$ is to introduce interactions that are commutable with the constraint terms. In this way, by preparing an initial state that satisfies the relevant constraint condition, we can execute the search among states that do not violate the constraint. For example, as discussed in Ref. 24, to map a typical combinatorial optimization problem, the traveling salesman problem (TSP) with N cities, into the Ising model, one prepares Ising spins on an $N \times N$ square lattice. The information about the distances between cities is embedded in the Ising interaction. In addition, two constraints are embedded: there can be only one up spin in each column (the number of cities that can be visited at a time is one) and there can be only one up spin in each row (each city can be visited only once). One possible interaction for $\hat{H}_1$ that is completely commutative with those constraint terms is the swap operator that exchanges all Ising spins in any two columns or rows, realized by preparing N direct products of the two-body Heisenberg interaction plus a constant term. For the TSP problem, it is easy to prepare an initial state that does not violate the constraint conditions, and

thus the state search can be performed only in the state space that satisfies the constraint conditions by using the QI search algorithm. Although finding an appropriate $\hat{H}_1$ is not always simple, especially when multiple constraints are simultaneously imposed, this strategy is expected to be useful because it reduces the degrees of freedom of the constraints to be considered.

The proposed method is "quantum-inspired" in the sense that we exploit the quantum interaction $\hat{H}_1$ to generate classical product states, and those states having higher energies are then truncated to keep the number of low-energy states manageable as in the Krylov subspace method.

As we have demonstrated, after repeatedly applying this procedure, the ground state as well as the low-energy states of the classical Ising Hamiltonian $\hat{H}_0$ are successfully obtained. A similar algorithm based on the same strategy can be applied to obtain the ground state of the quantum Hamiltonian $\hat{H} = \hat{H}_0 + \hat{V}_1$, where $\hat{H}_0$ are the classical Hamiltonian and $\hat{V}_1$ is the perturbatively small quantum Hamiltonian. It is a legitimate approximation in terms of perturbation theory to calculate the ground state by diagonalizing the Hamiltonian $\hat{H}$ in the Hilbert space spanned by a finite number of classical product states, which are expanded by applying $\hat{V}_1$ and are then truncated in accordance with their weights of contribution to the approximate ground state in the expanded Hilbert space.

Acknowledgments We would like to thank T. Shirakawa and M. Ohzeki for helpful comments. The work was partially supported by KAKENHI Nos. JP17K14359, JP18K03475, JP18H01183, JH20H01849, JP21K03395, JP21H03455, JP21H04446, and JP21H05191, and by JST PRESTO No. JPMJPR1911. This work was also supported by MEXT Q-LEAP Grant Number JPMXS0120319794 and the COE research grant in computational science from Hyogo Prefecture and Kobe City through Foundation for Computational Science. We are also grateful RIKEN for allowing us to use the computational resources of the HOKUSAI BigWaterfall supercomputing system.

Appendix: QI Search for Larger Systems and Comparison with PTMC Calculations

For practical use, it is important to verify that the QI search method can efficiently find the ground state in large systems up to $O(10^3)$. To this end, we need the reference data for the ground-state energy in large systems that cannot be treated by the brute-force method. Here, we employ the PTMC method,[27,39–42] which is well known as one of the best heuristic methods for searching the ground state of a system such as the classical Ising model described by the Hamiltonian $\hat{H}_0$ in Eq. (1).

Figure A·1 shows the ground-state energies obtained by the QI search method and the PTMC method for 120 different instances of the random coupling realizations in $\hat{H}_0$ with the system sizes $N = 200$, 600, and 1000. For the PTMC calculations, we adopt a large number of MC sweeps (2×10^5) and a comparable numerical condition described in Ref. 31. As shown in the figure, for the system size $N = 200$, the QI search with the input parameters $(L, K, I) = (N, N, N)$ finds the same ground-state energies as the PTMC method for 95 random coupling instances out of 120 instances, while for the remaining 25 random coupling instances, the QI search is trapped in metastable states with larger energies.

For $N = 600$, the success rate of the QI search finding the same ground-state energy as the PTMC method is reduced to 6/120 with the input parameters $(L, K, I) = (N, N, N)$, 9/120 with $(N, 2N, 2N)$, 18/120 with $(N, 5N, 5N)$, and 26/120 with $(N, 10N, 10N)$, showing a gradual improvement with increasing K and I. On the other hand, in the case of $N = 1000$, the QI search cannot find the ground-state energy consistent with the PTMC method for any of the 120 random coupling realizations, even when we set the input parameters $(L, K, I) = (N, 10N, 10N)$. These results suggest that a further increase in (L, K, I) or better tuning of the form of $\hat{H}_1$ is required to efficiently search the ground state in large systems.

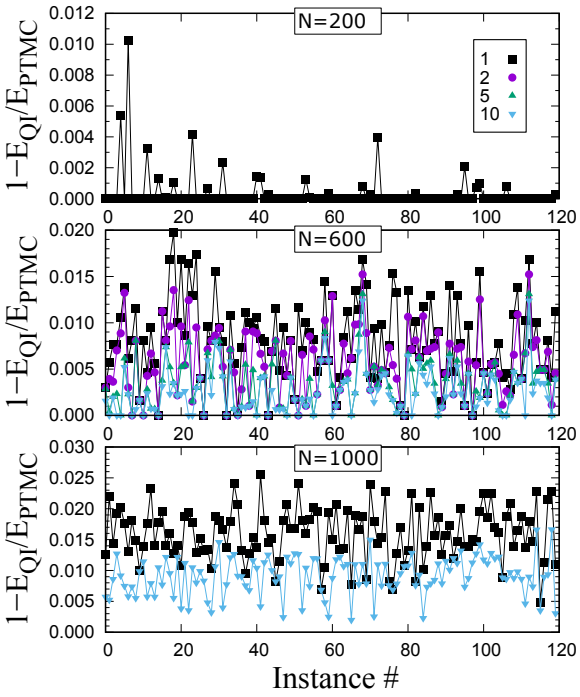

Fig. A·1. (Color online) Ground-state energies estimated by the QI search method ($E_{\rm QI}$) and the PTMC method ($E_{\rm PTMC}$) for 120 different instances of the random coupling realizations in $\hat{H}_0$ with $N = 200$, 600, and 1000. The different input parameters $(L, K, I) = (N, aN, aN)$ with $a = 1$, 2, 5, and 10 (indicated in the legend) are used for the QI search method. Note that the estimated energies $E_{\rm QI}$ and $E_{\rm PTMC}$ are both negative and thus $1 - E_{\rm QI}/E_{\rm PTMC} \geq 0$ implies $E_{\rm QI} \geq E_{\rm PTMC}$.

1) T. Kadowaki and H. Nishimori, Phys. Rev. E **58**, 5355 (1998).
2) T. Kadowaki, arXiv:quant-ph/0205020.
3) E. Farhi, J. Goldstone, S. Gutmann, J. Lapan, A. Lundgren, and D. Preda, Science **292**, 472 (2001).
4) R. Martoňák, G. E. Santoro, and E. Tosatti, Phys. Rev. E **70**, 057701 (2004).
5) S. Morita and H. Nishimori, J. Math. Phys. **49**, 125210 (2008).
6) A. Das and B. K. Chakrabarti, Rev. Mod. Phys. **80**, 1061 (2008).
7) M. Ohzeki and H. Nishimori, J. Comput. Theor. Nanosci. **8**, 963 (2011).
8) T. Albash and D. A. Lidar, Rev. Mod. Phys. **90**, 015002 (2018).
9) M. W. Johnson, M. H. S. Amin, S. Gildert, T. Lanting, F. Hamze, N. Dickson, R. Harris, A. J. Berkley, J. Johansson, P. Bunyk, E. M. Chapple, C. Enderud, J. P. Hilton, K. Karimi, E. Ladizinsky, N. Ladizinsky, T. Oh, I. Perminov, C. Rich, M. C. Thom, E. Tolkacheva, C. J. S. Truncik, S. Uchaikin, J. Wang, B. Wilson, and G. Rose, Nature **473**, 194 (2011).
10) V. S. Denchev, S. Boixo, S. V. Isakov, N. Ding, R. Babbush, V. Smelyanskiy, J. Martinis, and H. Neven, Phys. Rev. X **6**, 031015 (2016).

11) A. Lucas, Front. Phys. **2**, 5 (2014).
12) F. Barahona, J. Phys. A **15**, 3241 (1982).
13) Y. Fu and P. W. Anderson, J. Phys. A **19**, 1605 (1986).
14) M. Mezard, G. Parisi, and M. Virasoro, *Spin Glass Theory and Beyond* (World Scientific, Singapore, 1987) Lecture Notes in Physics Series.
15) K. Binder and A. P. Young, Rev. Mod. Phys. **58**, 801 (1986).
16) S. Kirkpatrick, C. D. Gelatt, and M. P. Vecchi, Science **220**, 671 (1983).
17) L. Zhou, S.-T. Wang, S. Choi, H. Pichler, and M. D. Lukin, Phys. Rev. X **10**, 021067 (2020).
18) P. Ehrenfest, Ann. Phys. **356**, 327 (1916).
19) M. Born and V. Fock, Z. Phys. **51**, 165 (1928).
20) J. Schwinger, Phys. Rev. **51**, 648 (1937).
21) T. Kato, J. Phys. Soc. Jpn. **5**, 435 (1950).
22) Y. Seki and H. Nishimori, Phys. Rev. E **85**, 051112 (2012).
23) Y. Susa, Y. Yamashiro, M. Yamamoto, and H. Nishimori, J. Phys. Soc. Jpn. **87**, 023002 (2018).
24) T. Huang, S. T. Goh, S. Gopalakrishnan, T. Luo, Q. Li, and H. C. Lau, arXiv:2103.10695.
25) Z. Strakoš and J. Liesen, *Krylov Subspace Methods Principles and Analysis* (Oxford University Press, Oxford, U.K., 2012) Numerical Mathematics and Scientific Computation.
26) Y. Hieida, K. Okunishi, and Y. Akutsu, Phys. Lett. A **233**, 464 (1997).
27) K. Hukushima and K. Nemoto, J. Phys. Soc. Jpn. **65**, 1604 (1996).
28) K. Hukushima, H. Takayama, and K. Nemoto, Int. J. Mod. Phys. C **7**, 337 (1996).
29) T. F. Rønnow, Z. Wang, J. Job, S. Boixo, S. V. Isakov, D. Wecker, J. M. Martinis, D. A. Lidar, and M. Troyer, Science **345**, 420 (2014).
30) M. Aramon, G. Rosenberg, E. Valiante, T. Miyazawa, H. Tamura, and H. G. Katzgraber, Front. Phys. **7**, 48 (2019).
31) I. Rozada, M. Aramon, J. Machta, and H. G. Katzgraber, Phys. Rev. E **100**, 043311 (2019).
32) D. Sherrington and S. Kirkpatrick, Phys. Rev. Lett. **35**, 1792 (1975).
33) M. Palassini and A. P. Young, Phys. Rev. Lett. **83**, 5126 (1999).
34) M. Palassini, J. Stat. Mech. **2008**, P10005 (2008).
35) J.-P. Bouchaud, F. Krzakala, and O. C. Martin, Phys. Rev. B **68**, 224404 (2003).
36) S. Boettcher, Eur. Phys. J. B **46**, 501 (2005).
37) S.-Y. Kim, S. J. Lee, and J. Lee, Phys. Rev. B **76**, 184412 (2007).
38) A. W. Sandvik, AIP Conf. Proc. **1297**, 135 (2010).
39) R. H. Swendsen and J.-S. Wang, Phys. Rev. Lett. **57**, 2607 (1986).
40) C. Geyer, in *Proceedings of the 23rd Symposium on the Interface*, ed. E. M. Keramidas (Interface Foundation, Fairfax Station, VA, 1991) p. 156.
41) M. Falcioni and M. W. Deem, J. Chem. Phys. **110**, 1754 (1999).
42) D. J. Earl and M. W. Deem, Phys. Chem. Chem. Phys. **7**, 3910 (2005).